IEEE Open Access Journal of Power and Energy

Received 3 February 2022; revised 4 June 2022 and 23 July 2022; accepted 13 September 2022.
Date of publication 5 January 2024; date of current version 1 March 2024.

Digital Object Identifier 10.1109/OAJPE.2023.3347972

Rolling Horizon Approach for Real-Time Charging and Routing of Autonomous Electric Vehicles

AVISHAN BAGHERINEZHAD[1] (Student Member, IEEE), MAHNOOSH ALIZADEH[2] (Senior Member, IEEE), AND MASOOD PARVANIA[1] (Senior Member, IEEE)

[1]Department of Electrical and Computer Engineering, The University of Utah, Salt Lake City, UT 84112 USA
[2]Department of Electrical and Computer Engineering, University of California at Santa Barbara, Santa Barbara, CA 93106 USA
CORRESPONDING AUTHOR: M. PARVANIA (masood.parvania@utah.edu)

ABSTRACT The adoption of autonomous electric vehicles (AEVs) offers an opportunity to decarbonize the transportation sector while eliminating the human errors in driving accidents. However, adopting AEVs may impose challenges to the operation of power distribution systems to ensure the availability of power for charging a growing number of AEVs at different times and locations. This paper takes an opportunistic look at this problem and develops a rolling horizon model for coordinating the operation of electric autonomous ride-hailing systems with power distribution systems. The proposed model incorporates the most recent real-time information and the future expected value of energy level, spatial and temporal location of AEV fleet, traffic data, and passenger demand. Using this data, the proposed model adopts a rolling horizon approach to optimize the routing of AEVs to serve spatio-temporal passenger demand across the transportation network, while optimizing the time and location of AEVs charging to ensure the availability of energy to serve the passenger demand, and satisfying the operational constraints of the power distribution system. The proposed model is implemented on a test transportation system, coupled with the IEEE 33-bus test power distribution system. The numerical results demonstrate the capability of the proposed model in ensuring the reliability and quality of service for both electric autonomous ride-hailing and power distribution systems.

INDEX TERMS Autonomous electric vehicle, ride-hailing services, power distribution system, vehicle charging and routing.

I. INTRODUCTION

A. BACKGROUND ON ELECTRIC AUTONOMOUS RIDE-HAILING

A VIABLE pathway to mitigate the impacts of fossil-fuel based transportation systems and associated environmental challenges is transportation electrification. According to [1], the transportation sector accounts for 24% of CO2 emissions globally. In response, nations around the world have passed legislation in support of transportation electrification that has resulted in a global number of 5.1 million electric vehicles (EVs) in 2019, a 61% expansion over the previous year [1]. The emergence of transportation network platforms, e.g., Lyft and Uber, have expanded the transit landscape to offer personalized, on-demand mobility from a ride-hailing service where public transit options are limited. Ride-hailing platforms offer a management and communication system through which transportation electrification can be expanded by the increased adoption of EVs. In order to achieve this, ride-hailing platforms have started multiple electrification initiatives to increase EVs in their fleet [2].

Ride-hailing connects passengers to potential drivers through web-based platforms [3]. Traditionally, drivers act independently in their pursuit of profit through passenger selection, driving hours, and charging location, which leads to ride-hailing platforms falling short in capturing the opportunities for service improvement through vehicles and operators' cooperation. However, recent advancements in the technology of self-driving EVs, also known as autonomous

electric vehicles (AEVs), offer opportunities for coordinated ride-hailing dispatch that would mitigate spurious vehicle trips and provide a higher quality of ride-hailing services. Moreover, high penetration of AEVs enables mitigating human error, which is responsible for 94% of all crashes in 2016 according to the National Highway Traffic Safety Administration [4]. The upcoming shift from human-operated fossil-fuel-based cars to AEVs is anticipated to reduce the operation cost of a vehicle by two to four times [5].

The adoption of electric autonomous ride-hailing platforms challenges the operating regimes of both ride-hailing systems and power distribution system (PDS). Robust operation of AEV fleet in a ride-hailing platform is achieved by a meticulous vehicle charging and routing strategy. However, the AEVs charging requirement may cause congestion in power distribution lines, and increase the line losses and bus voltage swings if proper coordination is not adopted [6]. To this end, the ride-hailing platform must have adequate insight on both ride-hailing and PDS states, i.e., the real-time traffic data, spatio-temporal status of AEVs, state of charge (SOC) of batteries, available charging stations, voltage level, and current flow magnitude.

B. LITERATURE REVIEW

In contrast to electron flow in a power distribution system, the vehicles in a transportation system cannot travel instantaneously from one point to another. Instead, a relatively long time is required for a vehicle to traverse a road which varies with the road's maximum capacity and time of day. Thus, the traffic flow at each road and each time interval is the accumulation of newly arriving AEVs and the existing AEVs and other vehicles on that road from previous time intervals. Connecting passengers to drivers in a ride-hailing platform is a specific instance of the vehicle routing problem (VRP), where the total traveled distance of a vehicle fleet with respect to customer satisfaction is minimized. Different variations of VRP are studied in the literature, such as pick up and delivery problems in [7], [8], [9], and [10], the VRP with time window where the customer must be visited within a given time window in [11], [12], and [13], and dynamic multi-commodity flow in [14], [15], and [16]. The VRP, often viewed as a network flow problem, is a dynamic problem in the real world, where static network flows fall short in capturing the spatio-temporal variations of the problem. In [9] and [10], routing of electric autonomous on-demand mobility considering the charging requirement is investigated; however, the interdependency of the transportation and power distribution systems is not considered. Also, in [9], the impact of traffic and the maximum capacity of roadways in the transportation network modeling is neglected, and in [10], it is assumed that there is a charging station at each node with no congestion constraints, which is incongruous with existing charging infrastructure conditions.

The impact of EV charging requirements on the power system operation is investigated in [17], [18], [19], and [20]. In [17], a two-stage model is proposed to manage the total charging requirement of EVs and curtail the load such that the reliable operation of the PDS is maintained. The proposed model alters the charging requirements of the EVs without considering the transportation system constraints and interdependent structure of the power and transportation systems. In [18], a stochastic security-constrained unit commitment coupled with a transportation system is proposed to determine the aggregated charging and discharging schedule of EVs such that power system operation cost is reduced and traffic congestion is alleviated. In [19], a multi-community user equilibrium model is presented to capture the interdependency of the power and traffic flow taking into account the marginal electricity price, fast charging stations location, and rational route selection of EVs while considering a generating unit at each bus of the power system. In [20], a planning model to determine the siting and sizing of EV charging stations considering the load expansion, power distribution, and transportation network constraints is proposed. In [21], a routing model for autonomous mobility on demand considering the charging constraints of AEVs is proposed, however, the proposed model does not consider the power distribution constraints and deliverability of the energy. In [22], the authors model the charging and routing of autonomous on-demand mobility considering the transportation and power transmission system constraints. The proposed economic dispatch model integrates the upper-level power transmission system constraints and does not take into account the implications of electric autonomous mobility charging requirements on the connected PDS in real-time operation. In [23], the authors investigate re-balancing and charging of autonomous mobility on demand considering the power distribution system. The model in [23], however, is for day-ahead operation that considers fixed routes for picking up and dropping off passengers, and does not integrate real-time traffic data, spatio-temporal passenger demand and power distribution load for charging and routing of AEVs.

Traditional ride-hailing systems aim at minimizing fuel, maintenance, and depreciation cost while maximizing the revenue received by dropping off passengers. However, recent advancement in AEVs, which are driven without a driver, is changing the ride-hailing paradigm by removing drivers' preference in the route and charging station selection. The electric autonomous ride-hailing (EAR) systems are considered customers of power distribution systems that demand energy to charge AEVs batteries. Therefore, the availability of energy to cater to the charging demand of AEVs and consequently adequacy of AEVs SOC to operate in a reliable manner is crucial. Although the proposed models in the literature tackle different aspects of EV integration in power system operation, the challenges imposed by the penetration of AEVs in ride-hailing systems and existing opportunities to provide energy flexibility spatially and temporally by proposing different optimization engines are not studied. More specifically, a clear gap remains in understanding the implications of the paradigm shift to electric

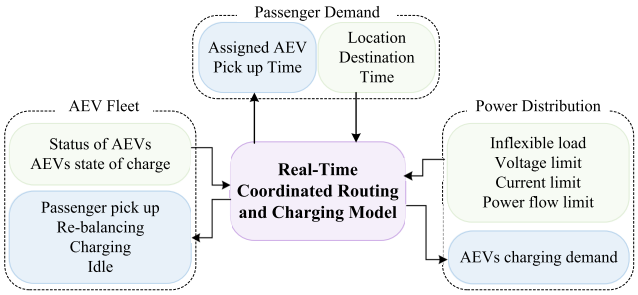

FIGURE 1. The real-time coordinated charging and routing model for AEVs.

autonomous mobility in the ride-hailing platforms on the real-time operation of power distribution systems. Moreover, there is a need to develop models to take the interdependent structure of power distribution and transportation systems into account and investigate the impact of high charging requirements of AEVs considering the mobility of AEVs to meet the charging demand spatially and temporally while respecting PDS constraints [24]. In this context, this paper aims at studying the real-time coordinated AEV charging and routing problem considering the operational constraints of both transportation and power distribution systems using an optimization-based framework.

C. CONTRIBUTION AND PAPER STRUCTURE

This paper proposes a rolling horizon approach for real-time charging and routing of AEVs in EAR systems co-optimized with power distribution system operation. The proposed model exchanges information between the passenger demand, AEV fleet, and the power distribution system, as illustrated in Fig. 1. The proposed model captures the interdependecies between the power distribution and electric autonomous ride-hailing systems, where the AEVs drive and re-balance across the transportation system to pick up passengers and charge the batteries at charging stations supplied by the power distribution system. Re-balancing AEVs refers to changing the location from one place to another in the ERA system for different purposes, i.e., meeting the future passenger demand, or charging. The proposed model utilizes the AEVs mobility to provide energy flexibility at different locations and times to the power distribution system while serving the passengers of the EAR system. In this context, the proposed coordinated charging and routing model re-balances the AEVs throughout the transportation system based on the real-time data on traffic and available charging flexibility at different stations to charge AEVs and guarantee the availability of energy to serve the passenger demand.

The proposed model, formulated as a relaxed mixed-integer second-order cone program (MISOCP), adopts a rolling horizon framework that receives and incorporates the most recent real-time information and the future expected value of energy level, spatial and temporal location of the AEV fleet, as well as the traffic data to determine the optimal charging and routing of AEVs. By considering a finite rolling horizon at each time step, the model can make decisions for the current time interval considering the variability of other parameters of the system in the future, e.g., traffic information, spatio-temporal passenger demand, and availability of plugs at charging stations. Therefore, at each rolling horizon the optimization engine reaches the optimal solution for the current interval, the binding interval, while considering the future predictions in the model. Although the decision of advisory intervals at each rolling horizon is not used directly, considering a rolling horizon enables the optimization engine to determine the binding interval solution such that the feasibility of the model for advisory intervals is ensured.

The rest of the paper is organized as follows: the modeling approach for the EAR infrastructure and the structure of the proposed rolling-horizon operation model are discussed in Section II. The EAR charging and routing problem formulation is presented in Section III. The simulation setup and numerical results are delineated in Section IV and conclusions are drawn in Section V.

II. REAL-TIME ELECTRIC AUTONOMOUS RIDE-HAILING

This section presents the proposed model for an interdependent EAR system and power distribution system. The transportation system is modeled by a directed graph $G^T = (\mathcal{N}, \mathcal{L}^T)$, where $\mathcal{N}$ and $\mathcal{L}^T$ are sets of nodes and roads in the transportation system. The charging infrastructure is located on a subset of the nodes in the transportation system, $\mathcal{N}^s \subset \mathcal{N}$. A set of AEVs, shown by $\mathcal{E}$, supply the spatio-temporal passenger demand of EAR system throughout the city. The passengers of the ride-hailing system are spatially and temporally distributed across the city with access to ride-hailing applications and the internet. The passenger demand varies by the time of day and spatial pattern of major access points throughout the transportation system, where commute needs from and to these locations are high. The spatio-temporal passenger demand is defined as the pick-up location $i \in \mathcal{N}$, and drop-off location $d \in \mathcal{N}$, respectively referred to as origin and destination in the model.

The PDS is also modeled by a graph $G^P = (\mathcal{B}, \mathcal{L}^P)$, where $\mathcal{B}$ and $\mathcal{L}^P$ are the sets of buses and lines in the power distribution system. The PDS caters to inflexible and flexible (spatio-temporal charging requirement of AEVs) loads in different buses of the power distribution system. The transportation nodes equipped with charging infrastructure are connected to adjacent buses in the power distribution system. In the AEV transportation system, AEVs travel across different nodes in which only a few of them are equipped with charging infrastructure. Thus, the charging opportunities of the AEVs are confined by parking in those nodes when they are not carrying passengers or re-balancing in the system.

The proposed model considers the future development of the passenger demand and power distribution load profiles by adopting the rolling horizon optimization approach. This approach opportunistically schedules the charging and routing of AEVs at each time considering the future passenger

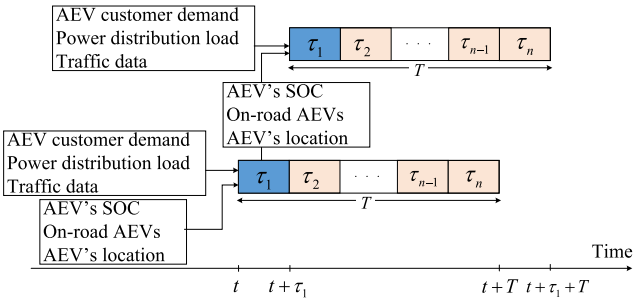

FIGURE 2. The proposed rolling horizon optimization approach for real-time coordinated charging and routing of electric autonomous ride-hailing systems.

demand in the transportation system and the corresponding spatio-temporal charging requirement in the power distribution system. Figure 2 illustrates an overview of the proposed rolling horizon optimization approach and the required input data. Each rolling scheduling horizon is divided to n segments, $T = [\tau_1, \tau_2, \ldots, \tau_n]$. The initial spatio-temporal passenger demand, AEVs locations, on-road AEVs, SOC of AEVs, and updated traffic and PDS data are fed into each rolling scheduling horizon, $[t, t+T]$, to co-optimize the charging and routing of AEVs. The first interval of each rolling horizon solution, τ_1 in Fig. 2, is the binding optimal decision variable while the rest, τ_2 to τ_n in Fig. 2, are advisory schedules. The binding decision variables of each rolling horizon are fed into the next scheduling horizon as the initial value of the parameters. Concatenating the binding decision variables of different rolling scheduling horizons generates the optimal real-time trajectories of variables during the scheduling horizon. The formulation of the proposed model is presented in Section III.

III. ELECTRIC AUTONOMOUS RIDE-HAILING CHARGING AND ROUTING CO-OPTIMIZATION MODEL

The proposed model for co-optimizing the charging and routing of electric autonomous ride-hailing considering the power distribution system is formulated in (1)-(29). The objective function of the proposed model is presented as follows:

$$\min \sum_{e,t}(\overline{E}_e - E_{e,t})\lambda_t^{pe} - \sum_{e,id,d,t} Z^p_{e,id,d,t}\lambda^{in} + \sum_{e,ij,d,t} Z^p_{e,ij,d,t} L_{ij,t}(\lambda^r + \lambda^m) + \sum_{e,ij,t} Z^r_{e,ij,t} L_{ij,t}(\lambda^p + \lambda^m). \tag{1}$$

The first term in (1) penalizes the deviation of AEVs' SOC from the maximum energy capacity by a factor λ_t^{pe} to ensure that there would be adequate energy stored in the AEV batteries to serve the transportation demand. This term correlates with the energy price to encourage AEVs to charge their batteries when the electricity price is low. The SOC of the AEVs is directly impacted by the amount of energy that AEVs request from the PDS to charge their batteries. Thus, by considering the SOC of batteries at each time interval in (1), the EAR system and PDS are coupled together. The second term in (1) calculates the revenue received by EAR system from dropping off the passengers, where the binary variable $Z^p_{e,id,d,t}$ indicates the occupancy statu of AEV on road id towards destination d, and λ^{in} is the corresponding incentive coefficient. The third and fourth terms in the second line of (1) minimize the energy and maintenance costs of AEVs traveling the distance $L_{ij,t}$ on road ij at time t, where the binary variable $Z^r_{e,ij,t}$ denote the status of AEV during re-balancing. The terms λ^r and λ^p respectively denote the price of consumed energy per mile for re-balancing and carrying passengers, and λ^m represents the maintenance cost of AEV. The objective function (1) is constrained by the transportation system and traffic constraints, AEV charging constraints as well as the power distribution constraints as discussed next.

A. TRANSPORTATION SYSTEM CONSTRAINTS

The traffic flow on road $ki \in \mathcal{L}^T$ at time t is equal to the total number of vehicles re-balancing and occupied with passengers, respectively shown by $N^r_{ki,t-1}$ and $N^p_{ki,t-1}$. In (2), the summation of AEVs on road $ki \in \mathcal{L}^T$ heading toward node $i \in \mathcal{N}$, either re-balancing or carrying passengers, plus the number of AEVs parked at node $i \in \mathcal{N}$, $N_{i,t-1}$, at time $(t-1)$ is equal to the number of parked AEVs at node $i \in \mathcal{N}$, plus the number of AEVs leaving node i through connecting roads either carrying a passenger or re-balancing at time t. Equations (3) and (4) present the re-balancing and carrying passengers flow of AEVs in line $ij \in \mathcal{L}^T$ at time t, respectively. The binary variables $Z^r_{e,ij,t}$ and $Z^p_{e,ij,d,t}$ are equal to 1 when AEV is respectively re-balancing and carrying a passenger from node i to node j, and are 0 otherwise. The spatio-temporal passenger demand balance of AEVs is ensured in (5) and (6). The initial passenger demand at node $i \in \mathcal{N}$ for destination $d \in \mathcal{N}$ at time t is denoted by $D^0_{i,d,t}$. The assignment of an AEV to pick up a passenger is represented by binary variable $X^p_{e,ij,d,t}$. The presence of traffic in the transportation system makes the required time to travel road $ij \in \mathcal{L}^T$ time dependent, $T_{ij,t}$. The second term in (6), captures the arrival of on-road AEVs carrying passengers at node i through connecting roads with destination d.

$$\sum_{ki\in\mathcal{L}^T}(N^r_{ki,t-1}+N^p_{ki,t-1})+N_{i,t-1} = N_{i,t} + \sum_{ij\in\mathcal{L}^T}(N^r_{ij,t}+N^p_{ij,t}), \tag{2}$$

$$\sum_e Z^r_{e,ij,t} = N^r_{ij,t}, \tag{3}$$

$$\sum_{e,d} Z^p_{e,ij,d,t} = N^p_{ij,t}, \tag{4}$$

$$\sum_{ij\in\mathcal{L}^T,e} X^p_{e,ij,d,t_1} = D^0_{i,d,t_1}, \tag{5}$$

$$\sum_{ij\in\mathcal{L}^T,e} X^p_{e,ij,d,t} = D^0_{i,d,t} + \sum_{ki\in\mathcal{L}^T,e} Z^p_{e,ki,d,t-1}(1 - Z^p_{e,ki,d,t}). \tag{6}$$

Constraint (7) ensures that an AEV is either re-balancing or occupied by a passenger on road $ij \in \mathcal{L}^T$ at time t. As the traffic and passenger demand data is updated, constraint (8) prevents going back and forth on a road. In (9), the status of AEV is equal to zero when AEV is at destination ($i = d$). Constraint (10) prevents unnecessary stops while carrying a passenger until the vehicle reaches the final destination node.

$$\sum_{ij,d} Z^p_{e,ij,d,t} + \sum_{ij} Z^r_{e,ij,t} \le 1, \tag{7}$$

$$Z^p_{e,ij,d,t-1} + Z^p_{e,ji,d,t} \le 1, \tag{8}$$

$$Z^p_{e,ij,d,t} = 0, \quad i = d, \tag{9}$$

$$\sum_{i} Z^p_{e,ij,d,t-1} \le \sum_{k} Z^p_{e,jk,d,t}, \quad j \ne d. \tag{10}$$

B. TRAFFIC DATA INTEGRATION

The real-time traffic data are integrated into the model by considering a maximum capacity and a travel time profile, $T_{ij,t}$, for each road. The density of a road is defined as the number of vehicles per unit length of the road in the transportation system. In (11), the number of vehicles on road $ij \in \mathcal{L}^T$ at time t (either re-balancing or carrying a passenger) is capped by $\mathrm{L}_{ij}\overline{\rho}_{ij}$, where $\overline{\rho}_{ij}$ and L_{ij} are respectively the maximum density during congestion and the length of the road $ij \in \mathcal{L}^T$. In (12), the AEV average speed (traveled distance divided by elapsed time) is constrained within the maximum and minimum speed limit of road ij, shown respectively by $\overline{V}_{ij}$ and $\underline{V}_{ij}$. The total number of AEVs at charging station $i \in \mathcal{N}^s$ at time t is constrained by maximum available charging plugs at the charging station, $\overline{N}^S_{s,t}$ in (13). Constraints (14) and (15) secure the minimum on-road time of AEVs, in which an AEV is on-road for $T_{ij,t+1}$ intervals when it starts the trip, assigned to carry a passenger or re-balance, at time $t+1$ from node i toward node j. The binary variable $X^r_{e,ij,t}$ is equal to 1 when AEV re-balances on road ij, and 0 otherwise.

$$0 \le N^r_{ij,t} + N^p_{ij,t} \le L_{ij}\overline{\rho}_{ij}, \tag{11}$$

$$\underline{V}_{ij} \le \frac{\mathrm{L}_{ij}}{T_{ij,t}} \le \overline{V}_{ij}, \tag{12}$$

$$N_{i,t} \le \overline{N}^S_{s,t}, \quad \forall i \in \mathcal{N}^s, \tag{13}$$

$$\sum_{\tau=t+1}^{\tau=t+1+T_{ij,t+1}} Z^p_{e,ij,d,\tau} \ge T_{ij,t+1}(X^p_{e,ij,d,t+1} - X^p_{e,ij,d,t}), \tag{14}$$

$$\sum_{\tau=t+1}^{\tau=t+1+T_{ij,t+1}} Z^r_{e,ij,\tau} \ge T_{ij,t+1}(X^r_{e,ij,t+1} - X^r_{e,ij,t}). \tag{15}$$

C. AEV CHARGING CONSTRAINTS

The operation of the EAR system relies on adequate charging of AEVs throughout the transportation network. In (16), if AEV is at node i the binary variable $X^L_{e,i,t}$ is equal to 1, and is 0 otherwise. Equation (17) keeps track of the SOC of AEV $e \in \mathcal{E}$ during scheduling horizon, where the battery charging and trip efficiency factors are represented by η^{ch} and η^{trip}, respectively. The stored energy in AEV batteries is capped by $\underline{E}_e$ and $\overline{E}_e$ in (18), respectively minimum and maximum capacity of the AEV batteries. Constraint (19) guarantees that there is enough energy to drive road $ij \in \mathcal{L}^T$ at time t. The AEV charging power is limited to charging plug power capacity if at station, and 0 otherwise, in (20). The parameter $\mathcal{M}$ is a $(\mathcal{N}^s \times \mathcal{N})$-dimensional incidence matrix, where component $M_{s,i}$ is 1 when charging station $s \in \mathcal{N}^s$ is located at node $i \in \mathcal{N}$ of the transportation system, and is 0 otherwise. The non-linear constraints (6), (16), and (20) are linearized using the method in [25].

$$X^L_{e,i,t} = \sum_{j,d} Z^p_{e,ji,d,t-T_{ji,t}} + \sum_{j} Z^r_{e,ji,t-T_{ji,t}} + X^L_{e,i,t-1}\Big(1 - \sum_{i,d} Z^p_{e,ji,d,t-T_{ji,t}} - \sum_{i} Z^r_{e,ik,t-T_{ij,t}}\Big), \tag{16}$$

$$E_{e,t+1} = E_{e,t} + \eta^{ch} P^{ch}_{e,t+1} - \eta^{trip}_t (Z^p_{e,ij,t+1,d} + Z^r_{e,ij,t+1}) L_{ij,t+1}, \tag{17}$$

$$\underline{E}_e \le E_{e,t} \le \overline{E}_e, \tag{18}$$

$$E_{e,t} - \eta^{trip}(X^p_{e,ij,t+1,d} + X^r_{e,ij,t+1})\mathrm{L}_{ij} \ge \underline{E}_e, \tag{19}$$

$$P^{ch}_{e,t} \le \overline{P}^{plug} M_{s,i} X^L_{e,i,t}\Big(1 - \sum_{ij} Z^p_{e,ij,d,t-T_{ij,t}} - \sum_{ij} Z^r_{e,ij,t-T_{ij,t}}\Big). \tag{20}$$

D. POWER DISTRIBUTION SYSTEM CONSTRAINTS

The operation of power distribution systems is modeled using (21)-(29):

$$P^G_t = \sum_{1y \in \mathcal{L}^P} P^L_{1y,t} + g_1 V^{sq}_{1,t}, \tag{21}$$

$$Q^G_t = \sum_{1y \in \mathcal{L}^P} Q^L_{1y,t} + b_1 V^{sq}_{1,t}, \tag{22}$$

$$\begin{aligned} &- P^D_{w,t} - \sum_e P^A_{e,w,t} = \sum_{wy \in \mathcal{L}} P^L_{wy,t} \\ &- \sum_{zw \in \mathcal{L}^P} (P^L_{zw,t} - r_{zw} I^{sq}_{zw,t}) + g_w V^{sq}_{w,t}, \end{aligned} \tag{23}$$

$$\begin{aligned} &- Q^D_{w,t} - \sum_e Q^A_{e,w,t} = \sum_{wk \in \mathcal{L}} Q^L_{wy,t} \\ &- \sum_{zw \in \mathcal{L}^P} (Q^L_{zw,t} - x_{zw} I^{sq}_{zw,t}) + b_w V^{sq}_{w,t}, \end{aligned} \tag{24}$$

$$V^{sq}_{w,t} - V^{sq}_{z,t} = -2(r_{zw} P^L_{zw,t} + x_{zw} Q^L_{zw,t}) + (r^2_{zw} + x^2_{zw}) I^{sq}_{zw}, \tag{25}$$

$$\underline{V^{sq}_w} \le V^{sq}_{w,t} \le \overline{V^{sq}_w}, \tag{26}$$

$$I^{sq}_{zw,t} \le \overline{I^{sq}_{zw}}, \tag{27}$$

$$V^{sq}_{w,t} I^{sq}_{zw,t} \ge P^2_{zw,t} + Q^2_{zw,t}, \forall t, \tag{28}$$

$$P^A_{e,w,t} = \sum_i P^{ch}_{e,t} X^L_{e,i,t} R_{w,i}. \tag{29}$$

The terms P^G_t and Q^G_t in (21) and (22) denote the active and reactive powers supplied by the upstream transmission system. The active and reactive power balance equations are formulated in (21)-(24), where $P^D_{w,t}$, $Q^D_{w,t}$, $P^A_{e,w,t}$, and $Q^A_{e,w,t}$

denote the active and reactive power distribution load, and active and reactive charging requirement of AEV e at bus w, respectively. The active and reactive power flow in line zw is denoted by $P^{L}_{zw,t}$ and $Q^{L}_{zw,t}$. The resistance and reactance of line zw, and the connected conductance and susceptance to bus w are respectively shown by r_{zw}, x_{zw}, g_w, and b_w. The voltage drop in line zw is formulated in (25), and the squared voltage $V^{sq}_{w,t}$ in (26) is confined within the squared minimum and maximum voltage thresholds $\underline{V^{sq}_{w}}$ and $\overline{V^{sq}_{w}}$. In (27), the squared current flow $I^{sq}_{zw,t}$ is constrained by the squared maximum current flow limit, $\overline{I^{sq}_{zw}}$. The non-convex AC-OPF problem can be relaxed as a rotated second-order cone constraint in (28), which encircles the equality in the optimal solution [26]. In (29), the charging requirements of AEVs at the charging station i at time t is mapped into the associated bus in the power distribution system. The $(N \times B)$-dimensional incidence matrix $\mathcal{R}$ maps the power distribution buses to the nodes of the transportation system, where $R_{w,i}$ is 1 if node $i \in \mathcal{N}$ of the transportation system is connected to bus $w \in \mathcal{B}$ of the power distribution system, and 0 otherwise.

The proposed model (1)-(29) is a MISOCP, which is a convex optimization problem that can be solved using commercial solvers, as shown next in the simulation results next.

IV. SIMULATION RESULTS

The proposed model for coordinated charging and routing of EAR system with the PDS is implemented on a test real-world transportation system and the IEEE 33-bus test PDS [27]. A portion of the transportation system of Salt Lake City, UT is used as the test transportation system, which includes actual routes in major interstates, state highways, important destinations (i.e., University of Utah campus, Salt Lake City Airport, etc.), and available EV charging stations. The transportation system includes 13 nodes, $\mathcal{N} = [n_1, \ldots, n_{13}]$, 16 roads, and 7 charging stations, $\mathcal{N}^s \subset \mathcal{N} = [s_1, \ldots, s_7]$. Roadway capacity is defined as the rate of vehicles that traverse a point or uniform section of a roadway during a given period of time under existing roadway conditions [28]. The roadway capacities and congestion are determined by the Utah Department of Transportation average annual hourly volume dataset for the Salt Lake City metro area [29]. The hourly values are scaled down by 12 and linear interpolation is applied to align the hourly data with the 5-minute operation time in the model.

The PDS caters the inflexible and flexible load (spatio-temporal charging demand of AEVs) of the customers. The IEEE 33-bus PDS [30] is spatially mapped to the transportation system to highlight the interconnection of the two systems. The spatial connectivity of charging stations in the Salt Lake City metro area and associated transportation nodes and PDS buses is shown in Table 1. Each charging station is equipped with five 50 kW charging plugs that are used by AEVs in ride-hailing system. The charging requirement of conventional electric vehicles is set to zero. The real-time load of CAISO for January 16, 2019, is scaled down to 3,715kW and 2,300kVAr for active and reactive peak power

TABLE 1. Connectivity map of the power and transportation networks.

Charging Station	S1	S2	S3	S4	S5	S6	S7
Transportation Node	n1	n2	n3	n4	n6	n7	n13
Power Distribution Bus	b26	b23	b29	b3	b19	b11	b16

TABLE 2. Case study assumptions.

Cases	Transportation & Power Distribution Model	Power distribution load	Traffic
Case 1-1	Uncoordinated	Off peak	Light
Case 1-2	Uncoordinated	Morning peak	Heavy
Case 2-1	Coordinated	Off peak	Light
Case 2-2	Coordinated	Morning peak	Heavy

of the test PDS [31]. The minimum and maximum voltage threshold are 0.9 pu and 1.1 pu in the system.

In order to investigate the impacts of traffic and PDS status (e.g., the magnitude of inflexible power load, voltage and current flow) on charging and routing of AEVs in interdependent PDS and EAR system, two case studies each with two scenarios are studied, as defined in Table 2. In Case 1, the impacts of uncoordinated charging and routing of AEVs on the PDS is investigated, in which the EAR operator only considers the transportation system constraints without coordinating with PDS. In Case 2, the coordinated charging and routing of AEVs considering both transportation and PDS constraints is investigated. In this case, the spatio-temporal passenger demands and AEV charging demands are supplied such that the constraints of EAR system and PDS are met. The optimal charging and routing of AEVs vary based on the traffic and PDS load. For this reason, the impacts of off-peak PDS load and light traffic in scenario 1, and PDS morning peak load and heavy traffic in scenario 2, are investigated. The real-time simulation study is implemented in a 30 minutes rolling horizon, every 5 minutes for 24 intervals (2 hours) to depict the traffic and PDS load impacts. The proposed model is implemented in a GAMS environment, on a desktop computer with a 3.6-GHz i7 processor and 16 GB of RAM in which the average computational time for each run is 27.68 and 49.36 seconds for Cases 2-1 and 2-2, respectively.

The average 5-minute intervals required to travel a road during scheduling horizon and AEV passenger demand are presented in Table 6 in Appendix. The required time to drive through different roads in the transportation system differs upon location and time of day. The average 5-minute interval required to travel a road in scenario 1 is less than scenario 2 in most of the roads, indicating lighter traffic in the transportation system. A subset of the transportation system nodes are selected randomly as the initial location of ten AEVs, $\{n_1, n_2, n_4, n_7, n_{10}, n_{11}\} \subset \mathcal{N}$. The maximum energy capacity of AEVs is 50 kWh, in which the initial SOC is considered 50% of that. The charging efficiency of AEVs is considered 80% and the rate of energy discharge on road is 0.32 kWh/mile [32].

TABLE 3. Operation cost of electric autonomous ride-hailing system.

Cost ($)	Case 1-1	Case 1-2	Case 2-1	Case 2-2
Carrying Passenger	20.91	22.30	20.91	22.30
Re-balancing	0.81	1.39	0.81	1.39
A-EV Charging	43.05	60.70	54.63	45.30
Maintenance and Depreciation	3.48	3.79	3.48	3.79

TABLE 4. Comparison of different models.

	Random model	Geedy model	Optimization model
Supplied passenger demand (%)	23	64	100
Energy consumption cost ($)	7.34	15.91	21.72
Maintenance & deprecation cost ($)	1.17	2.55	3.48
Requested charging energy (kWh)	30	4	242.67

A. COST ANALYSIS

The operation cost of the EAR system comprises the cost of consumed energy for carrying passengers and re-balancing in the transportation system, the cost of charging AEVs batteries at the charging stations, and the maintenance and deprecation cost as shown in Table 3. The maintenance and depreciation cost of AEVs is $0.16/mile [22]. The energy and charging costs are calculated based on the constant rate of $0.22/kWh [33]. The light traffic creates more opportunities for AEVs to re-balance and charge the batteries by spending less time on-road carrying passengers. However, heavy traffic in scenario 2, Cases 1-2 and 2-2, results in increasing the energy cost for carrying passengers and re-balancing compared to Cases 1-1 and 2-1, respectively. Further, there are fewer charging opportunities in Case 2-2 due to PDS constraints and morning peak load which results in less charging cost for AEVs compared to Case 2-1. The maintenance and deprecation cost is calculated based on the traveled miles for each case study, where the heavy traffic in scenario 2 results in rerouting the AEVs and increasing the travelled miles and consequently maintenance and deprecation cost compared to scenario 1.

B. PERFORMANCE ANALYSIS

The proposed model is compared with random and greedy models in Table 4. In the random model, AEVs take random decisions to serve passengers, re-balance, and charge in pursuit of profit in the EAR system. However, the low percentage of the served passengers in the random model highlights the missed opportunities in adopting such a model to meet the passenger demand and reduce the associated costs. In the greedy model, the AEVs prioritize re-balancing and serving passengers in the EAR system, and only charge when the AEV energy hits the minimum energy threshold. Although the greedy model meets 64% of the passenger demand, the myopic behavior of such an algorithm increases the AEVs energy cost. However, the proposed coordinated optimization model fully serves the passenger demand while optimizing the AEVs charging and considering the power distribution system constraints. The required energy to charge AEVs in random and greedy models is significantly lower than that in the optimization model, which showcases the shortsighted behavior of these models.

C. CHARGING REQUIREMENT OF THE EAR SYSTEM

The total charging requirement of the AEVs in charging stations is shown in Fig. 3. The charging profile of AEVs and consequently charging profile of each station is dependent on traffic, passenger demand, location of charging stations, and available charging capacity based on PDS status. In Cases 1-1 and 1-2, the power distribution system constraints are not considered in the determining the optimal charging of the AEVs, therefore the charging power profile of s_2, s_4, s_6, and s_7 are significantly different from Cases 2-1 and 2-2, highlighting the impact of power distribution system constraints, as shown in Fig. 3. Further, the charging profile of s_2, s_4, and s_7 are altered in Fig. 3-d compared to Fig. 3-c, which highlights the impact of the power distribution load on optimal charging of AEVs. For instance, charging station s_7 is connected to a sensitive PDS bus and the coordinated co-optimization model tailors the charging profile of s_7 in Cases 2-1 and 2-2 such that the PDS operation constraints and EAR system requirements are satisfied, as shown by the black curve in Fig. 3. In Case 2-2 the inflexible morning peak load of PDS results in less charging flexibility and a more tailored charging profile at station s_4 compared to Case 2-1. Further, the charging profile of s_4 in Cases 1-1 and 2-1 is different from Cases 1-2 and 2-2 which highlights the impacts of power distribution load and transportation system traffic on AEVs charging profiles. As discussed above, the charging profile of the AEVs is determined such that the stations are not overloaded and power distribution constraints are not violated.

D. EAR RESOURCE ALLOCATION AND SPATIO-TEMPORAL STATUS OF AEVs

In the proposed real-time charging and routing problem AEVs have four modes: carrying a passenger, re-balancing, parking idle, and charging AEVs batteries at a charging station, in which Table 5 showcases the average percentage of the time allocated to each mode in all cases. The main objectives of AEVs is to serve the passengers of EAR system and recharge in the remaining time to ensure the quality of service. The average time that AEVs are carrying passengers is almost 40% of the scheduling time in all cases, which signifies the role of coordinated scheduling of EAR system and PDS to take advantage of the remaining 60% of the time to ensure the operation reliability of EAR system and PDS. Therefore, the coordinated charging and routing of AEVs in Cases 2-1 and 2-2 re-balances and charges the batteries of AEVs such that the average idle time of AEVs is significantly reduced and average charging time is increased compared to Cases 1-1 and 1-2, respectively.

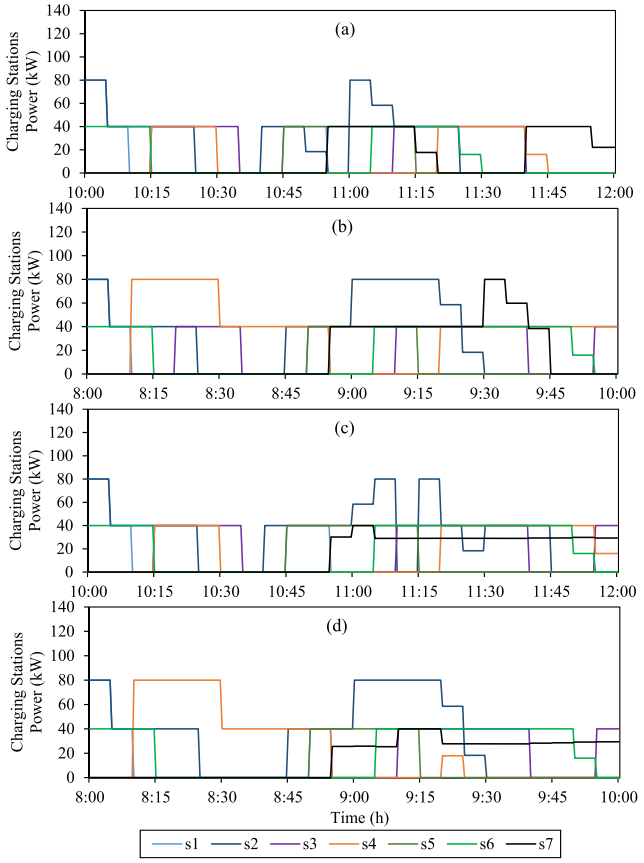

FIGURE 3. The total charging requirement of AEVs in the transportation system in: a) Case 1-1, b) Case 1-2, c) Case 2-1, and d) Case 2-2.

TABLE 5. EAR resource allocation percentage in case studies.

	Carrying passenger	Re-balancing	Charging	Idle
Case 1-1	37.50	2.92	25.83	33.75
Case 1-2	39.58	5.00	35.42	20.00
Case 2-1	36.25	2.92	40.42	20.42
Case 2-2	39.58	5.00	42.92	12.50

The spatio-temporal status of an AEV, e_2, for Cases 2-1 and 2-2 is illustrated in Fig. 4. Initially e_2 is located at node n_1 of the transportation system with a charging station, and there exist a passenger demand to travel from n_1 to n_3, as in Table 6-B in Appendix. Therefore, in Case 2-1 e_2 picks up the passenger at the first interval, purple circle at time 10 AM in Fig. 4-a, and drops off the passenger at n_3. Next, the battery of e_2 is charged for 20 minutes at n_3 to satisfy the minimum energy threshold constraint of the EAR system and then re-balanced to n_1 to meet a future demand at 11.05 AM. However, in Case 2-2 in Fig. 4-b, e_2 is assigned to charge the batteries at the current location and then pick up the spatio-temporal passenger demand with destination n_2 at 8.10 AM. In Cases 2-1 and 2-2, the same AEV is assigned to different tasks which highlights the impacts of

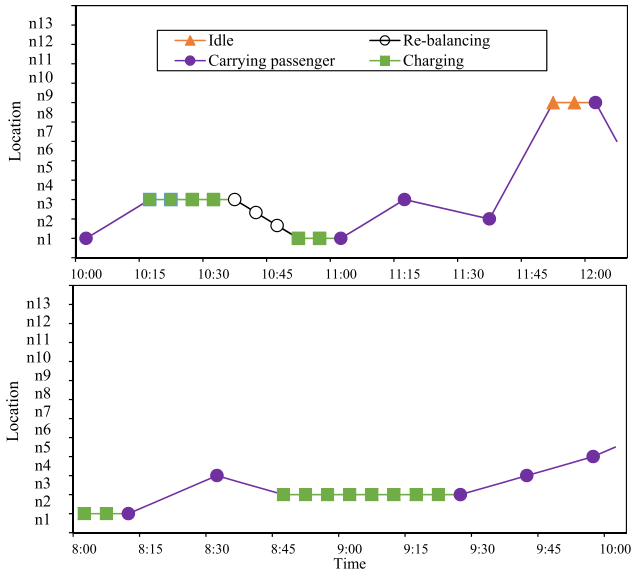

FIGURE 4. The spatio-temporal status of AEV e_2: a) Case 2-1 and b) Case 2-2.

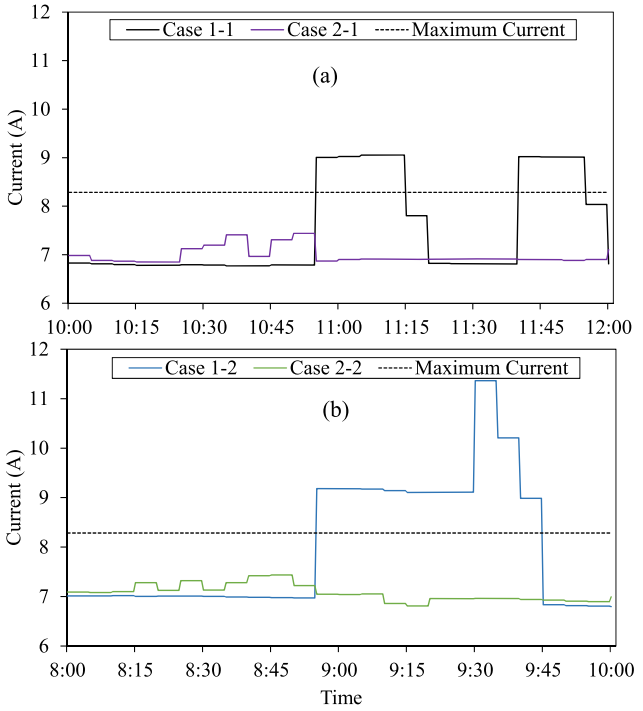

FIGURE 5. Current profile from b_{16} to b_{17} in the power distribution system.

the transportation and PDS status on charging and routing of AEVs in EAR operation.

E. CURRENT PROFILES OF POWER DISTRIBUTION SYSTEM

The EAR system is dependent on the PDS to cater the charging requirements of AEVs. Figure 5 depicts the current flow

TABLE 6. a) Average required 5-minute intervals to travel a road, b) Spatio-temporal passenger demand of ride-hailing system.

(A)

From	To	Scenario 1	Scneario 2
n1	n3	3	3.46
n2	n3	3	3.25
n2	n8	3	3.25
n3	n4	3	3.25
n3	n9	3	3.29
n4	n5	2	2
n4	n10	3	3
n5	n6	3.46	3.83
n5	n7	3	3
n6	n13	3	3
n7	n11	2	2
n8	n9	2.13	2
n9	n10	3	3
n10	n11	2.25	2.25
n11	n12	3	3
n12	n13	4	4

(B)

Time	Origin	Destination
t1	n1	n3
	n2	n5
t3	n1	n2
t4	n7	n6
t5	n11	n13
t6	n2	n9
t7	n4	n2
t9	n10	n3
t10	n10	n7
t12	n1	n8
t14	n5	n13
t15	n5	n4
t16	n6	n13
t18	n2	n7
t19	n8	n3
t21	n3	n5
t24	n8	n3

from PDS bus b_{16} to b_{17}, in which the black dashed line represents the maximum flow capacity of the line. In Cases 1-1 and 1-2, the uncoordinated charging and routing of AEVs results in violation of the current flow in the PDS, black and blue curves in Fig. 5. The charging station s_7 is connected to node b_{16} that indicates the explicit impact of the charging profile of this station, black curve in Fig. 3, on the current flow. However, in Cases 2-1 and 2-2, the charging and routing of AEVs in EAR system is altered to prevent current flow violations, as shown in green and purple curves in Fig. 3. Therefore, the real-time charging and routing of AEVs in interdependent EAR system and PDS ensures the reliable operation of PDS and consequently EAR system.

V. CONCLUSION

This paper proposed a model to devise real-time spatio-temporal charging and routing schedule for AEVs in the interdependent power distribution and EAR systems. The proposed rolling horizon approach meticulously captures the twisted structure of interdependent systems to re-balance the AEVs in order to serve the passengers and charge AEVs considering the operational constraints of EAR system and PDS. The proposed real-time charging and routing model for AEVs is tested on a transportation system coupled with IEEE 33-bus power distribution system. The simulation results indicates that the real-time charging and routing model ensures the quality of service in the EAR system operation by reducing spurious trips and taking advantage of the idle time of AEVs to re-balance and charge the batteries. Further, the proposed model determines the deliverable energy at each charging station spatially and temporally based on the PDS operational constraints, while the naive uncoordinated model violates the PDS constraints and jeopardizes the reliable operation of both PDS and EAR system. The simulation results demonstrate the efficiency of the proposed rolling horizon approach in incorporating the most recent traffic data, passenger demand, and PDS constraints to optimize the charging and routing profile of AEV fleet in varying real-time EAR system and PDS condition. The proposed real-time charging and routing model sheds light on the existing opportunities for cooperation of PDS and EAR system while adopting cost-effective and reliable strategies for scheduling the AEVs.

APPENDIX
TEST SYSTEM DATA

The traffic data and spatio-temporal passenger demand of the EAR system used in the simulations are presented here. Table 6-A denotes the average 5-minute intervals required to travel a road during the scheduling horizon in scenarios 1 and 2, respectively light and heavy traffic. For instance, it takes three 5-minute intervals, 15 minutes, on average to travel from n_1 to n_3 in scenario 1. The spatio-temporal AEV passenger demand is depicted in Table 6-B. The spatio-temporal AEV passenger demand is defined by the pick-up and drop-off locations, respectively denoted as origin and destination over the scheduling horizon, $t1$ to $t24$.

REFERENCES

[1] *IEA Global EV Outlook 2019*. Accessed: 2023. [Online]. Available: www.iea.org/publications/reports/globalevoutlook2019/

[2] P. Slowik, L. Fedirko, and N. Lutsey, "Assessing the ride-hailing company commitments to electrification," Int. Council Clean Transp., Tech. Rep., 2019. [Online]. Available: https://theicct.org/wp-content/uploads/2021/06/EV_Ridehailing_Commitment_20190220.pdf

[3] M. Moran. (2016). *Transportation Network Companies*. [Online]. Available: https://policy.tti.tamu.edu/wp-content/uploads/2017/03/TTI-PRC-TNCs-SBC-031417.pdf

[4] USDOT Releases. (2016). *Fatal Traffic Crash Data*. NHTSA. [Online]. Available: https://www.nhtsa.gov/press-releases/usdot-releases-2016-fatal-traffic-crash-data

[5] J. Arbib and T. Seba, "Rethinking transportation 2020–2030," *RethinkX*, vol. 143, p. 144, May 2017.

[6] A. Palomino and M. Parvania, "Advanced charging infrastructure for enabling electrified transportation," *Electr. J.*, vol. 32, no. 4, pp. 21–26, May 2019.

[7] S. N. Parragh, K. F. Doerner, and R. F. Hartl, "A survey on pickup and delivery problems: Part II: Transportation between pickup and delivery locations," *J. Für Betriebswirtschaft*, vol. 58, no. 2, pp. 81–117, Jun. 2008.

[8] S. Pelletier, O. Jabali, and G. Laporte, "The electric vehicle routing problem with energy consumption uncertainty," *Transp. Res. B, Methodol.*, vol. 126, pp. 225–255, Aug. 2019.

[9] F. Boewing, M. Schiffer, M. Salazar, and M. Pavone, "A vehicle coordination and charge scheduling algorithm for electric autonomous mobility-on-demand systems," in *Proc. Amer. Control Conf. (ACC)*, Jul. 2020, pp. 248–255.

[10] R. Iacobucci, B. McLellan, and T. Tezuka, "Optimization of shared autonomous electric vehicles operations with charge scheduling and vehicle-to-grid," *Transp. Res. C, Emerg. Technol.*, vol. 100, pp. 34–52, Mar. 2019.

[11] M. Schneider, "The vehicle-routing problem with time windows and driver-specific times," *Eur. J. Oper. Res.*, vol. 250, no. 1, pp. 101–119, Apr. 2016.

[12] M. Keskin, G. Laporte, and B. Çatay, "Electric vehicle routing problem with time-dependent waiting times at recharging stations," *Comput. Oper. Res.*, vol. 107, pp. 77–94, Jul. 2019.

[13] A. Y. S. Lam, Y.-W. Leung, and X. Chu, "Autonomous-vehicle public transportation system: Scheduling and admission control," *IEEE Trans. Intell. Transp. Syst.*, vol. 17, no. 5, pp. 1210–1226, May 2016.

[14] A. Hall, S. Hippler, and M. Skutella, "Multicommodity flows over time: Efficient algorithms and complexity," *Theor. Comput. Sci.*, vol. 379, no. 3, pp. 387–404, Jun. 2007.
[15] R. Iglesias, F. Rossi, K. Wang, D. Hallac, J. Leskovec, and M. Pavone, "Data-driven model predictive control of autonomous mobility-on-demand systems," in *Proc. IEEE Int. Conf. Robot. Autom. (ICRA)*, May 2018, pp. 6019–6025.
[16] M. Tsao, D. Milojevic, C. Ruch, M. Salazar, E. Frazzoli, and M. Pavone, "Model predictive control of ride-sharing autonomous mobility-on-demand systems," in *Proc. Int. Conf. Robot. Autom. (ICRA)*, May 2019, pp. 6665–6671.
[17] X. Lu, S. Xia, W. Gu, K. W. Chan, and M. Shahidehpour, "Two-stage robust distribution system operation by coordinating electric vehicle aggregator charging and load curtailments," *Energy*, vol. 226, Jul. 2021, Art. no. 120345.
[18] Y. Sun, Z. Chen, Z. Li, W. Tian, and M. Shahidehpour, "EV charging schedule in coupled constrained networks of transportation and power system," *IEEE Trans. Smart Grid*, vol. 10, no. 5, pp. 4706–4716, Sep. 2019.
[19] W. Wei, L. Wu, J. Wang, and S. Mei, "Network equilibrium of coupled transportation and power distribution systems," *IEEE Trans. Smart Grid*, vol. 9, no. 6, pp. 6764–6779, Nov. 2018.
[20] X. Wang, M. Shahidehpour, C. Jiang, and Z. Li, "Coordinated planning strategy for electric vehicle charging stations and coupled traffic-electric networks," *IEEE Trans. Power Syst.*, vol. 34, no. 1, pp. 268–279, Jan. 2019.
[21] R. Zhang, F. Rossi, and M. Pavone, "Model predictive control of autonomous mobility-on-demand systems," in *Proc. IEEE Int. Conf. Robot. Autom. (ICRA)*, May 2016, pp. 1382–1389.
[22] F. Rossi, R. Iglesias, M. Alizadeh, and M. Pavone, "On the interaction between autonomous mobility-on-demand systems and the power network: Models and coordination algorithms," *IEEE Trans. Control Netw. Syst.*, vol. 7, no. 1, pp. 384–397, Mar. 2020.
[23] A. Estandia et al., "On the interaction between autonomous mobility on demand systems and power distribution networks—An optimal power flow approach," *IEEE Trans. Control Netw. Syst.*, vol. 8, no. 3, pp. 1163–1176, Sep. 2021.
[24] A. Bagherinezhad, M. M. Hosseini, and M. Parvania, "Real-time coordinated operation of power and autonomous electric ride-hailing systems," *IEEE Trans. Smart Grid*, vol. 14, no. 3, pp. 2214–2225, May 2023.
[25] M. Parvania and M. Fotuhi-Firuzabad, "Integrating load reduction into wholesale energy market with application to wind power integration," *IEEE Syst. J.*, vol. 6, no. 1, pp. 35–45, Mar. 2012.
[26] M. Farivar and S. H. Low, "Branch flow model: Relaxations and convexification—Part II," *IEEE Trans. Power Syst.*, vol. 28, no. 3, pp. 2565–2572, Aug. 2013.
[27] *Modified IEEE 123-Bus Test Power Distribution System for Hierarchical Energy Storage Operation*. Accessed: 2023. [Online]. Available: https://usmart.ece.utah.edu/test-systems-and-data-ai/
[28] S. Hoogendoorn and V. Knoop, "Traffic flow theory and modelling," in *The Transport System and Transport Policy: An Introduction*, 2013, pp. 125–159.
[29] UDOT Transportation. (2018). *Monthly Hourly Volume Reports*. [Online]. Available: https://www.udot.utah.gov/connect/business/traffic-data/
[30] M. E. Baran and F. F. Wu, "Network reconfiguration in distribution systems for loss reduction and load balancing," *IEEE Trans. Power Del.*, vol. 4, no. 2, pp. 1401–1407, Apr. 1989.
[31] (Jan. 2019). *California ISO Open Access Same-Time Information System*. [Online]. Available: http://oasis.caiso.com
[32] *Department of Energy*. Accessed: 2023. [Online]. Available: https://afdc.energy.gov/vehicles/electric_emissions_sources.html
[33] C. Harto, "Electric vehicle ownership costs: Today's electric vehicles offer big savings for consumers," Consumer Rep., Tech. Rep., Oct. 2020. [Online]. Available: https://advocacy.consumerreports.org/wp-content/uploads/2020/10/EV-Ownership-Cost-Final-Report-1.pdf